Bull Earthquake Eng (2007) 5:303–323
DOI 10.1007/s10518-007-9032-7

ORIGINAL RESEARCH PAPER

Nonlinear numerical method for earthquake site response analysis I— elastoplastic cyclic model and parameter identification strategy

Fernando Lopez-Caballero · Arezou Modaressi-Farahmand Razavi · Hormoz Modaressi

Received: 13 February 2006 / Accepted: 23 January 2007 / Published online: 30 June 2007

Abstract This paper, along with its companion paper, presents the importance of the adequate soil behaviour model to simulate earthquake site response analysis. An elastoplastic model taking into account the elementary necessary plastic mechanisms such as progressive friction mobilization, Coulomb type failure, critical state and dilatancy/contractance flow rule, is used. However, one of the obstacles in the use of elastoplastic models in the everyday design processes for evaluation of the seismic soil response is the difficulty in identifying their parameters. In this paper, a methodology to identify a coherent set of parameters of the elastoplastic model for a given type of soil is presented. The strategy behind the decision making process proposed here is based on the use of minimum physical and easily measurable properties of the soil to directly provide or indirectly assess the required model parameters.

Keywords Constitutive model · Cyclic loading · Elastoplastic · Parameter identification · Liquefaction

1 Introduction

To simulate numerically seismic soil response, two approaches can be considered: the equivalent-linear approach and a truly non-linear elastoplastic modelling. The variation of shear modulus and material damping ratio with shear strain, known as G–γ and D–γ curves, has been known to be a significant feature of the soil behaviour submitted to cyclic loading since the pioneer works by Seed and Idriss [1970]. This observation resulted in the equivalent-linear approach that has been extensively used since then.

F. Lopez-Caballero (✉) · A. Modaressi-Farahmand Razavi
Laboratoire MSS-Mat CNRS UMR 8579, Ecole Centrale Paris, Grande Voie des Vignes, 92295 Châtenay-Malabry Cedex, France

H. Modaressi
Development Planning and Natural Risks Department, BRGM, BP 6009, 45060 Orléans Cedex 2, France

Even though its shortcomings have been repeatedly enumerated in the past, it has become the major tool in practical engineering applications due to its simplicity. On the other hand, the development of cyclic elastoplastic constitutive models for soils in the late 1970s and early 1980s has opened a new horizon for soil dynamics studies, (e.g. Prévost and Hoeg 1975; Ghaboussi and Dikmen 1978; Aubry et al. 1982 among others).

The information concerning the capability of these models in representing the variation of the shear modulus and the damping ratio in a wide range of shear strain, namely from 10^{-6} to 10^{-2} is scarce. Pande and Pietruszczak [1986] compared several constitutive models and reported that almost all of them, except those based directly on this property, were inefficient in reproducing this feature of soil behaviour. In this paper, we will give some numerical results showing that it is possible to simulate realistic G–γ and D–γ curves using an elastoplastic model.

The use of models based on the elastoplasticity theory is more suitable than equivalent-linear approach as they represent a rational mechanical process. In this kind of model, parameters should be chosen so that they are closely related to the rheology that describes the material properties at various strain levels. In some cases these rheological models do not necessarily have physical parameters. Sometimes there are indirect parameters that cannot be measured in the laboratory.

Thus, one of the obstacles in using such models is the difficulty in identifying their parameters. In addition, the lack of knowledge of soil properties is common in seismic studies and unfortunately, the cost of laboratory and in situ tests is quite expensive, so a complete geotechnical description of a site is very rare.

The elastoplastic model implemented in *CyberQuake* [Modaressi and Foerster, 2000] is used here and a methodology to identify the model parameters with a minimum laboratory data is proposed. This model is a derivation of the ECP elastoplastic models (also known as Hujeux's model) developed, refined and enhanced by Aubry and co-workers since the early 1980s [Aubry et al. [1982], Hujeux [1985] for the 3D cyclic behaviour, Aubry et al. [1990] for the interface behaviour]. Mellal [1997] integrated and used the present model for seismic site effects studies.

The strategy developed in this paper is based on the extensive work of the authors in this field and it can be generalized to all of the ECP family models. It is based on the use of easily measurable soil properties. The model's parameter identification methodology is developed for both clays and sands. As the G–γ and D–γ curves are largely used for the material identification in seismic analyses, we focus our work on such results. Thus, the objective of the soil identification is to obtain the elastoplastic model parameters resulting in a given set of G–γ and $D-\gamma$ curves measured in a shear test.

2 Formulation of the elastoplastic constitutive model

The cyclic *CyberQuake* model is written for laterally infinite parallel soil layers, where a one-dimensional geometry can be considered. However, the three dimensional kinematics assumptions integrate the complete displacement field. If x, y and z represent the reference axes in which the seismic motion is described, with z perpendicular to the soil layers, the three displacement components will vary only with respect to the

z axis if:

$$\underline{u}(z) = \underline{u}_x(z) + \underline{u}_y(z) + \underline{u}_z(z),$$

where $\underline{u}_i$ represents the component of the displacement along i direction.

On the potential shear plane with normal vector $\underline{n}$, the displacement can be presented as :

$$\underline{u}(z) = \underline{u}_t(z) + u_n(z) \cdot \underline{n},$$

where $\underline{u}_t$ designates the resultant of the displacements on the plane which defines the shear direction. Thus, the shear ($\underline{\gamma}$) and the normal (ε) strains are :

$$\underline{\gamma}(z) = \frac{\partial \underline{u}_t}{\partial z} = \frac{\partial \underline{u}_x}{\partial z} + \frac{\partial \underline{u}_y}{\partial z}$$
$$\varepsilon(z) = \frac{\partial u_n}{\partial z}.$$

In fact, the simple geometry consideration is usually an inherent feature of simplified methods. The principal step for simplified models is to introduce important aspects of the soil behaviour, such as strain shearing and/or pore-pressure build-up induced by the cyclic loading during earthquakes. Moreover, the seismic motion in the multilayer system is adequately represented considering a plane plastic shear mechanism.

The saturated soil skeleton is considered as a mixture of solid grains and the interstitial water. The behaviour of the solid skeleton is derived assuming the principle of effective stress as proposed by Terzaghi, where the total stress tensor ($\underline{\underline{\sigma}}$) is split in two components: the effective stress tensor ($\underline{\underline{\sigma}}'$) and the pore pressure (p). Where $\underline{\underline{\sigma}} = \underline{\underline{\sigma}}' - p \cdot \underline{\underline{I}}$ with $\underline{\underline{I}}$ the identity second order tensor. In this paper the mechanics of continuous media sign convention is adopted (i.e. compression negative).

This principle is valid as far as the solid grain compressibility is much smaller than the compressibility of the solid skeleton. We also assume that the pore pressure variation does not induce any deformation of the grains.

The effective stress (respectively strain) vector can be decomposed into normal and tangential components: σ' (respectively ε) and $\underline{\tau}$ (respectively $\underline{\gamma}$).

Modeling the elastic behaviour

In the very small strain range, soil behaviour is reversible. However, the elastic properties of the soil depend on the stress state. Assuming an isotropic elastic behaviour, the effective stress and strain rates are related as follows:

$$\begin{aligned} \dot{\sigma}' &= E^*(\underline{\underline{\sigma}}')\ \dot{\varepsilon}^e \\ \underline{\dot{\tau}} &= G(\underline{\underline{\sigma}}')\ \underline{\dot{\gamma}}^e, \end{aligned} \tag{1}$$

where E^* and G are the constrained and shear modules.

Modeling the elastoplastic behaviour

The yield function of the constitutive model presented here may be considered as a generalization of the Coulomb Friction law, in which some aspects such as the

dependency on the state of compactness and the evolving friction mobilization, similar to those used in ECP family models (Aubry et al. 1982, 1990; Hujeux 1985), are included. It represents a shearing on a plane and incorporates dilatancy-contractance in the direction normal to that plane. Therefore, the model is a derivation of the 3D model with some improvements. A vectorial formulation of the constitutive model permits plastic coupling effects between shearing and the plastic volumetric strain to be taken into account. The model is written in terms of effective stresses. Fundamental aspects of soil behaviour such as evolving plasticity, dilatancy and contractance, softening and hardening and cyclic hysteretic behaviour are included.

Following the incremental elastoplasticity theory, the rate of total strain is decomposed into reversible and irreversible parts:

$$\begin{cases} \dot{\varepsilon} = \dot{\varepsilon}^e + \dot{\varepsilon}^p \\ \underline{\dot{\gamma}} = \underline{\dot{\gamma}}^e + \underline{\dot{\gamma}}^p, \end{cases} \tag{2}$$

where $(\varepsilon^p, \underline{\gamma}^p)$ are normal and shear plastic strains on the surface normal to the wave propagation direction. The dot designates derivation with respect to time. Hence, combining (1) and (2) gives:

$$\begin{aligned} \dot{\sigma}' &= E^*(\dot{\varepsilon} - \dot{\varepsilon}^p) \\ \underline{\dot{\tau}} &= G\,(\underline{\dot{\gamma}} - \underline{\dot{\gamma}}^p). \end{aligned} \tag{3}$$

Both monotonous and cyclic loadings can be defined by a yield surface as follows:

$$f(\sigma', \underline{\tau}, \varepsilon^p, r) = \|\underline{\tau}^c\| + \sigma' \cdot F \cdot |r^c|, \tag{4}$$

where $\|\underline{a}\| = (\underline{a} \cdot \underline{a})^{1/2}$ and $|a|$ designates the absolute value of a. $r^c = r - r_o$ and $\underline{\tau}^c = \underline{\tau} - \frac{\sigma' F}{\sigma'_o F_o}\underline{\tau}_o$. The index o corresponds to the value of the variable at the latest loading reversal during the cyclic loading. The above formulation is advantageous as it can be applied to cyclic as well as monotonous (primary) loading, where $\underline{\tau}_o$ and r_o will be zero.

Isotropic hardening is taken into account by means of F and r. The function F permits to control the isotropic hardening associated with the plastic volumetric strain, whereas r accounts for the isotropic hardening generated by plastic shearing. It represents progressive friction mobilization in the soil and reaches its maximum value at perfect plasticity. F can be expressed as follows:

$$F = 1 - b \ln\left(\frac{\sigma'}{\sigma_c}\right), \tag{5}$$

with σ_c, the critical effective stress:

$$\sigma_c = \sigma_{\text{co}} \exp(-\beta\, \varepsilon^p). \tag{6}$$

The parameter b controls the form of the yield surface and varies from 0 to 1, passing from a Coulomb type surface to a Cam-Clay one (Fig. 1). A kinematical hardening is introduced during the loading-unloading cycles through the internal variable r. This latter is related to the plastic shear strain as follows:

$$r(\gamma^p) = r_o + (r_m - r_o)\left(\frac{|\gamma^p - \gamma_o^p|}{\frac{|r_m - r_o|}{E_p} + |\gamma^p - \gamma_o^p|}\right)^{n_r} \tag{7}$$

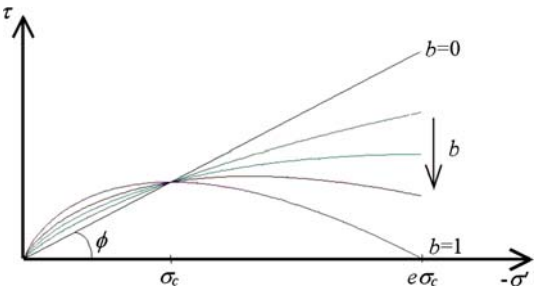

Fig. 1 Influence of parameter b on the yield surface shape

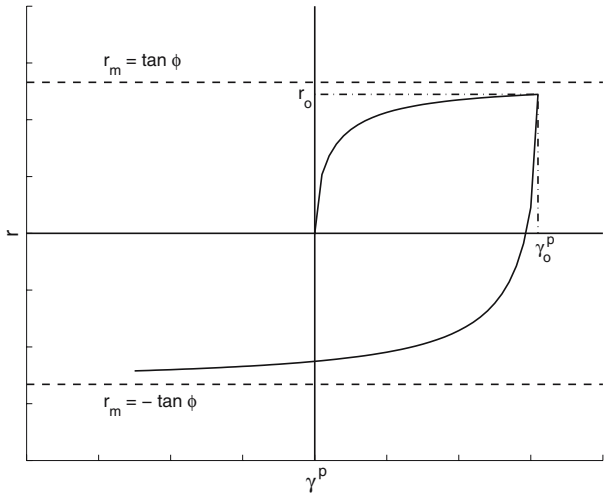

Fig. 2 Loading/unloading cycle

with:

$$r_m = \begin{array}{ll} \tan\phi' & \text{load/reload} \\ -\tan\phi' & \text{unload} \end{array},$$

where ϕ' is the friction angle at the critical state; γ^p is the plastic shear strain accumulated during the shearing ($\gamma^p = \int_0^t \|\underline{\dot{\gamma}}^p\| dt$); γ_o^p is the plastic shear strain accumulated at the very beginning of the loading until the last loading/reloading($\gamma_o^p = \int_0^{t_0} \|\underline{\dot{\gamma}}^p\| dt$) and n_r is a numerical parameter which guarantees a smooth evolution towards perfect plasticity (Fig. 2). E_p is the plastic modulus which governs the evolution of shear strains.

When the plastic strains grow dramatically in the soil, the function r reaches its maximal value r_m asymptotically:

$$\lim_{\gamma^p \to +\infty} r = r_m \text{ or } \lim_{\gamma^p \to +\infty} \|\underline{\tau}\| = -\sigma' F |r_m|. \tag{8}$$

Plastic volumetric strains associated with plastic shear strains are evaluated using a Roscoe-type dilatancy rule (Schofield and Wroth 1968):

$$\begin{aligned} \dot{\varepsilon}^p &= \dot{\lambda}^p \Psi_v \\ \underline{\dot{\gamma}}^p &= \dot{\lambda}^p \underline{\Psi}_d, \end{aligned} \tag{9}$$

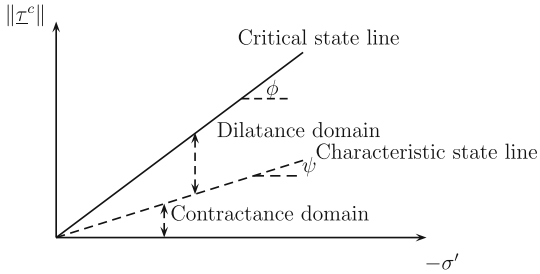

Fig. 3 Critical state and chacteristic state lines

where $\dot{\lambda}^p$ is the plastic multiplier.

$$\begin{aligned} \Psi_v &= -\alpha_\psi\ \zeta(r)\left(\tan\psi + \frac{\|\underline{\tau}^c\|}{\sigma'}\right) \\ \underline{\Psi}_d &= \partial_{\underline{\tau}} f\ =\ \frac{\underline{\tau}^c}{\|\underline{\tau}^c\|} \end{aligned} \tag{10}$$

ψ is the characteristic angle, defining the limit between dilatancy and contractance of the material (Fig. 3). $\zeta(r)$ has been introduced to control pore-pressure or volumetric strain evolution. It is zero for very low strains, equal to unity for large strains and varies from 0 to 1 for the intermediate range of strains. The parameter α_ψ is a constant parameter which enhances the model's performances. Set to zero, the plastic contractance or dilatance can be inhibited. In all our computations the unit value has been adopted.

$$\zeta(r) = \begin{cases} 0 & \text{if} \quad |r - r_o| < r_{\text{hys}} \qquad \text{elastic domain} \\ \left(\dfrac{|r - r_o| - r_{\text{hys}}}{r_{\text{mob}} - r_{\text{hys}}}\right)^2 & \text{if} \quad r_{\text{hys}} < |r - r_o| < r_{\text{mob}} \quad \text{hysteretic domain} \\ 1 & \text{if} \quad r_{\text{mob}} < |r - r_o| < 1 \qquad \text{mobilized domain} \end{cases} \tag{11}$$

with:

$$\begin{aligned} r_{\text{hys}} &= |r_m - r_o| \left(\frac{\gamma^{\text{hys}}}{\dfrac{|r_m - r_o|}{E_p} + \gamma^{\text{hys}}}\right)^{n_r} \\ r_{\text{mob}} &= |r_m - r_o| \left(\frac{\gamma^{\text{mob}}}{\dfrac{|r_m - r_o|}{E_p} + \gamma^{\text{mob}}}\right)^{n_r} \end{aligned} \tag{12}$$

Plastic coupling

Because of the plasticity mechanism, there are two types of coupling between different components of the seismic motion. The first concerns the two in plane components as the yield function depends of the amplitude of the shear stress, implying the interdependence of the plastic strain vectors and thus the shear stress and strain evolution in both directions. The second coupling links the normal and the in plane movements. Due to Eqs. 9 and 10, the induced increment of normal plastic strain is proportional to the amplitude of the increment of the shear strain : $\dot{\varepsilon}^p = \Psi_v \| \dot{\underline{\gamma}}^p \|$. Moreover, the

Table 1 Parameter classification according to their estimation method

	Rigidity and hardening	State	Behaviour domains
Directly measurable	Elasticity υ_s, υ_p [a] Plasticity β	ϕ', ψ $\sigma_{co}/\sigma', \rho$	$\gamma^{ela}, \gamma^{hys}$
Non-directly measurable	E_p, α_ψ, n_r	b	γ^{mob}

[a]In earthquake engineering, shear and compression wave velocities are usually used. If the mass density of the material is known, the elastic modulus E^* and G can be estimated

increments of the shear and normal stresses depend on the increment of the plastic shear strain vector in the plane (Eq. 3). This explains importance of taking into account all the components of shear strain. To these direct coupling effects, we can add the role of normal strain (normal stress) on the evolution of the yield function which controls the amplitude of the shear strains.

In practice, the computations of the seismic soil motion are carried out with each component of the input motion separately (i.e. each horizontal or vertical component). The coupling due to plasticity prohibits such individualized computations and enforces the need to perform computations with three components of the input motion simultaneously.

3 Elastoplastic constitutive model parameters

As already mentioned, the parameters of the model concern both the elastic and plastic behaviour of the soil (Table 1). The model parameters are classified according to their estimation method. From this point of view, the parameters used in the elastoplastic model are separated into two categories: those that can be directly measured either *in situ* or in the laboratory and those which cannot be directly measured.

3.1 Determination of directly measurable parameters

3.1.1 Elastic parameters

The isotropic elasticity assumption imposes the following relation between the shear and compression wave velocities and the Poisson's ratio ν: $(\upsilon_p/\upsilon_s)^2 = 2(1-\nu)/(1-2\nu)$. It shows that only two of the above three parameters have to be determined. When shear wave velocity measurement is not available, it can be estimated by: $\upsilon_s^2 = G_{max}/\rho$, where G_{max} is the maximum shear modulus measured at small strains and ρ is soil density.

3.1.1.1 Clays. Laboratory test data suggest that the maximum shear modulus G_{max} is a function of the void ratio e, the over-consolidation ratio OCR and the mean effective stress σ' (Hardin 1978; Vucetic and Dobry 1991; Kramer 1996; Kallioglou et al. 1999). Empirical relations can be used to determine this parameter according to the soil type. Figure 4 shows a comparison between the shear modulus obtained with different relations (Hardin 1978; Kokusho et al. 1982; Anastasiadis and Pitilakis 1996; Kallioglou et al. 1999; Santos 1999) for a normally consolidated clay at $\sigma' = 100$ kPa

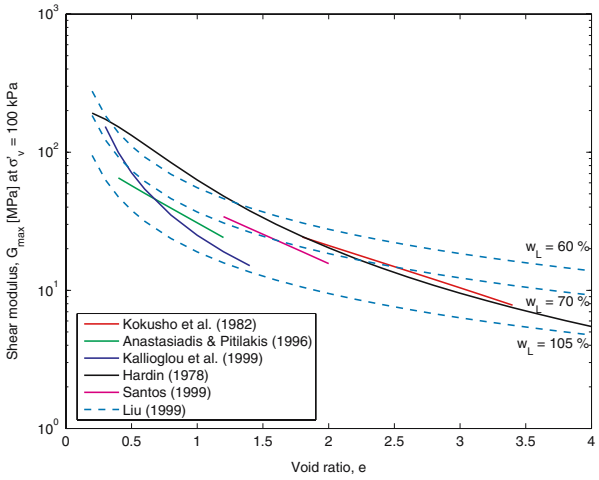

Fig. 4 Comparison of different relationships given for the maximum shear modulus

as a function of voids ratio e. For the overconsolidated clays, an additional multiplying parameter of the type OCR^k can be used. k is a factor depending on the plasticity index I_p, such that for I_p between 0 and 100% k varies from 0 to 0.5 (Hardin 1978).

3.1.1.2 Sands. As in clays, the maximum shear modulus $G_{\max}$ of sands can be expressed as a function of the void ratio e and the mean effective stress σ'. After Kohata et al. [1997], the variation of maximum modulus as a function of the confinement pressure obtained for different tested sands and gravels is very close. Thus, we propose to use the following relationship (Iwasaki et al. 1978) for the sand:

$$G_{\max} = 900\,\frac{(2.17-e)^2}{1+e}\,\sigma'^{0.4}\,p_a^{0.6}. \tag{13}$$

3.1.2 Plastic compressibility modulus β

The plastic compressibility modulus β can be expressed in terms of the λ parameter of the Cam-Clay model using the following relationship:

$$\beta \simeq \frac{1+e}{\lambda} \tag{14}$$

λ represents the slope of the virgin consolidation line of an isotropic compression test expressed in the $(e - \ln\sigma')$ plane. This parameter is related to the compression index C_c through: $C_c = 2.3\lambda$.

3.1.2.1 C_c and e for Clays.

For a normally consolidated clay, the following relation exists between the voids ratio e and the vertical effective stress σ': $e = e_0 - C_c \log(\sigma')$. Different authors propose a correlation between I_p and C_c (Biarez and Hicher 1994; Bardet 1997). In this paper, we use the correlation given by Biarez and Favre [1972], $C_c = 0.009(w_L - 13)$ where w_L is the liquidity limit. The strategy for the determination of e knowing the effective vertical stress is shown in Fig. 5, where, as it can be seen, e is equal to $G_S w_L/100$ for $\sigma' = 7$ kPa and $G_S w_p/100$ for $\sigma' = 1$ MPa, where G_S is the soil specific gravity.

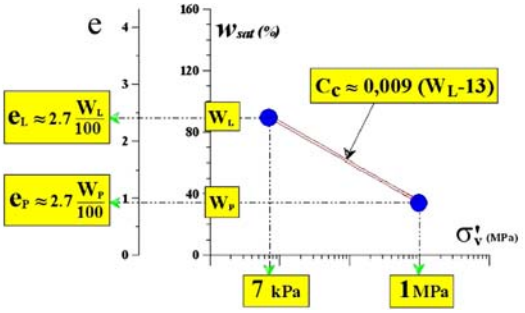

Fig. 5 The slope and the position of the oedometric compressibility curve for normally consolidated clays (Biarez and Favre [1972])

3.1.2.2 C_c for Sands. Saim [1997] proposes a correlation between C_c and the minimum and maximum void ratios $e_{\min}$ and $e_{\max}$ for sands, where the relative density D_r is equal to 0 for $\sigma'_v = 100\,\text{kPa}$ and 1 for $\sigma'_v = 5\,\text{MPa}$ at critical state. When the void ratio measurement is not available, it can be estimated by some correlations relating the $e_{\min}$ and $e_{\max}$ of sandy materials with respect to their grain size distribution (Biarez and Hicher [1994]).

In another approach, Hicher and Rahma [1994] propose a more general relation (Eq. 15) to obtain the β-value, by using a large sandy soil database. Thus parameter β-is given by the following relationship:

$$\beta = 2.3(1+e)\,\frac{\beta_{\text{norm}}}{I_e}. \tag{15}$$

I_e is the consistance index ($I_e = e_{\max} - e_{\min}$) and β_{norm} is given as:

$$\begin{aligned} \beta_{\text{norm}} &= \log P'c_{\max} - \log P'c_{\min}, \\ \log P'c_{\max} &= -4\log U_c - 7.5 \cdot e_{\min} + 4.75 \cdot I_e + 7.1 \pm 0.3, \\ \log P'c_{\min} &= -12\log C_z - 4.7 \cdot e_{\max} + 9.71 \cdot I_e + 2.2 \pm 0.5. \end{aligned} \tag{16}$$

U_c is the uniformity coefficient (d_{60}/d_{10}), where d_i designates the diameter of the grains representing i%, C_z is the coefficient of curvature ($d_{30}^2/d_{60} \cdot d_{10}$). $P'c_{\max}$ and $P'c_{\min}$ are the mean effective stress for $e_{\min}$ and $e_{\max}$, respectively.

3.1.3 Determination of ϕ' and ψ

For clays, Biarez and Hicher [1994] give a correlation between the friction angle ϕ' and the Plasticity Index I_p. In this correlation ϕ' decreases from 32° to 20° when I_p varies from 5 to 65% following this relationship:

$$\phi' = 44.5 \left(\frac{1}{I_p}\right)^{0.17}. \tag{17}$$

Favre [1980] gives the following relationship for the friction angle of sands:

$$\phi' = 31.5° + \phi_D + \phi_F + \phi_{U_c}, \tag{18}$$

where ϕ_D, ϕ_F and ϕ_{U_c} are used to account for granulometric features such as grain size, angularity and grain size distribution, respectively. The sum of these coefficient values varies in the range of ±2.5°.

As already mentioned, ψ represents the limit between contracting and dilating behaviours in sands, which is known as the "*phase transformation state*" or "*quasi-steady state*" (Ishihara et al. 1975; Ishihara 1993) The value of this parameter may be equal or less than ϕ'. In the case of clays, $\psi = \phi'$ can be chosen.

3.1.4 Initial state parameters

In the *CyberQuake* model, the initial state of the soil is given by the compaction ratio $\sigma_{\text{co}}/\sigma'$. This parameter represents the position of the critical state pressure σ_{co} with respect to the initial pressure σ'. If we neglect the elastic volumetric strain, σ_{co} can be defined as the pressure in the critical state line corresponding to the same void ratio as the initial pressure (σ'). The $\sigma_{\text{co}}/\sigma'$ ratio is a function of the initial density of the soil and the position of the initial void ratio with respect to the critical state line in the $(e - \ln \sigma')$ plane.

Thus, in the case of clays, this ratio remains constant for a given OCR at different initial pressures. Nevertheless, for sands, σ_{co} remains constant for a given D_r at different initial pressures. This parameter can be estimated by using different factors proposed to characterize both the response of clays and sands.

For clays, the compaction ratio can be estimated by the following relationship:

$$\frac{\sigma_{\text{co}}}{\sigma'} = \frac{Su}{\sigma' \tan \phi'}, \tag{19}$$

where S_u is the undrained shear strength ($S_u = (\sigma'_1 - \sigma'_3)/2 = \tau_{\max}$). For sands, it can be obtained using the following expression:

$$\frac{\sigma_{\text{co}}}{\sigma'} = \exp\left(-2.3\frac{\psi_{BJ}}{C_c}\right) \tag{20}$$

ψ_{BJ} is the "*state index*" parameter given by Been and Jefferies [1985].

3.2 Determination of non-directly measurable parameters

As the Cam-Clay yield surface represents the behaviour of clays better, while the Mohr-Coulomb is more adapted for sands, the value of b is determined with respect to this consideration (i.e. $b \simeq 0.1$–0.2 for sands and $b = 1.0$ for clays). The parameter n_r has been chosen equal to 0.5 for all cases.

3.2.1 Behaviour domains

The parameters γ^{ela}, γ^{hys} and γ^{mob}, are very important in liquefaction studies. They enable the decomposition of soil behaviour into pseudo-elastic, hysteretic and mobilized domains. These parameters control the degradation hysteresis and the water pore-pressure change in undrained conditions or the volumetric change in drained conditions. γ^{ela}, which takes very small values, defines the elastic domain in which no plastic shear strain occurs. γ^{hys} defines the plastic shear strain beyond which volumetric effects appear under shearing. This latter effect evolves according to relation 11.

To estimate γ^{hys} and γ^{mob}, a strain controlled cyclic shear (SCCS) test can be simulated in order to find the *volumetric threshold shear strain* γ_{tv} (Dobry et al. 1982; Vucetic 1994. In order to study the influence of these parameters in the model

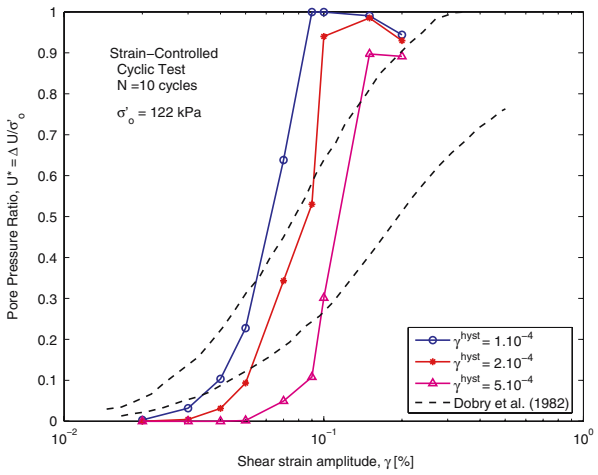

Fig. 6 Effect of variation of γ^{hys} in the model response of a strain controlled cyclic shear (*SCCS*) test. Comparison with Dobry et al. [1982] curves

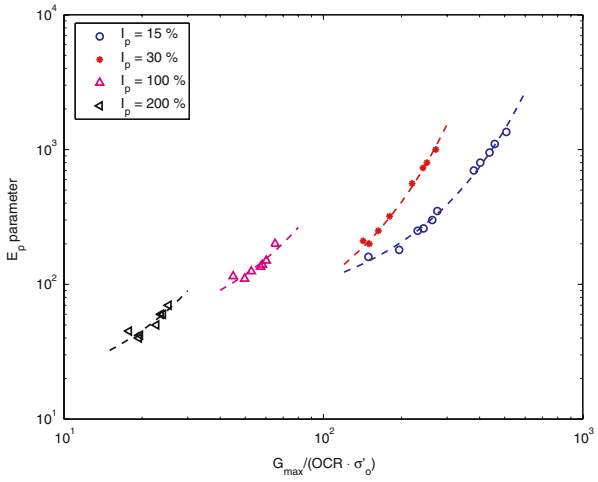

Fig. 7 Variation of E_p parameter as a function of G_{max}, OCR and σ' for different I_p-values (Case of clays)

response, three undrained SCCS tests are simulated (Fig. 6) and only the value of γ^{hys} is changed. According to this figure, the variation of γ^{hys} value modifies the γ_{tv} obtained.

3.2.2 Plasticity modulus of rigidity E_p

The parameter E_p governs the evolution of the yield surface towards total plastic mobilization. It will be determined in order to match the G–γ and D–γ curves for each type of soil. Several authors have summarized such curves (Kokusho 1980; Seed et al. 1986; Sun et al. 1988; Vucetic and Dobry 1991; Ishibashi and Zhang 1993; Darendeli 2001), according to the material type. As it is a conceptual example in this part of the work, the compiled curves of Vucetic and Dobry [1991] and those of Kokusho [1980] have been used as "measured" curves for clays and sands, respectively.

In order to study the influence of several features of soil behaviour on the E_p parameter, cyclic shear tests at different initial states have been simulated for both

Table 2 Values of coefficients of relations 21 and 22 to estimate the values of E_p parameter

Clay			Sand		
$I_p(\%)$	C_1	χ_{cl}	$D_r(\%)$	C_2	χ_{san}
15	57.1	6.414×10^{-3}	10	2,256	$-1.7\ 10^{-3}$
30	31.0	1.295×10^{-2}	20	1,895	$-2.1\ 10^{-3}$
100	31.0	2.681×10^{-2}	50	2,613	$-5.8\ 10^{-3}$
200	11.7	6.800×10^{-2}			

clays and sands. Using a statistical analysis of used data (Fig. 7), we can propose the following relationship to estimate the E_p-value for clays and sands (Eqs. 21 and 22), respectively:

$$E_p = C_1 \exp\left(\chi_{cl} \frac{G_{\max}}{\sigma' \cdot OCR}\right), \tag{21}$$

$$E_p = C_2 \exp\left(\chi_{san} \frac{G_{\max}}{\sigma_{\text{co}}}\right), \tag{22}$$

where C_1, χ_{cl} and C_2, χ_{san} are factors depending on the I_p and D_r, respectively (Table 2).

Finally, the whole methodology for the determination of elastoplastic model parameters for clays and sands is summarized in Figs. 8 and 9. As can be noted in these figures, for a given soil profile, the knowledge of one state parameter (i.e. OCR for clays and D_r for sands) and one parameter independent of the soil arrangement (i.e. Liquidity Limit of clays w_L and $e_{\min}$ and $e_{\max}$ for sands) is enough to obtain a set of model parameters, which can probably be refined if complementary data are available.

4 Model response for laboratory tests

In order to validate the proposed methodology and the coherence of the obtained set of parameters, we have studied clay and sand behaviours at different initial states (i.e. different values of σ' and OCR or D_r). The constitutive model parameters are then obtained by simulating the monotonic and cyclic tests.

4.1 Tests for clays

The model parameters were determined as described above and the undrained strain-controlled monotonous and cyclic direct simple shear tests were simulated. These tests were made for an $I_p = 15\%$ clay at three initial states and different OCR-values (i.e. 1.0, 2.0 et 3.0). The confining pressures (σ') used are 64, 70 and 189 kPa. Figure 10 shows the model prediction for the variation of $G/G_{\max}$ and the variation of damping ratio (D) with the cyclic shear strain γ for the undrained strain-controlled cyclic direct simple shear test. These curves are compared with the modulus reduction curve and the damping ratio for $I_p = 15\%$ clay given by Vucetic and Dobry [1991]. The shear modulus (G) obtained by the elastoplastic model is in good accordance with the given curve, though the model overestimates the damping for high-shear strains.

In order to define the different states of the clay (i.e. different OCR values), undrained monotonic simple shear tests are simulated. Figure 11 shows the results of

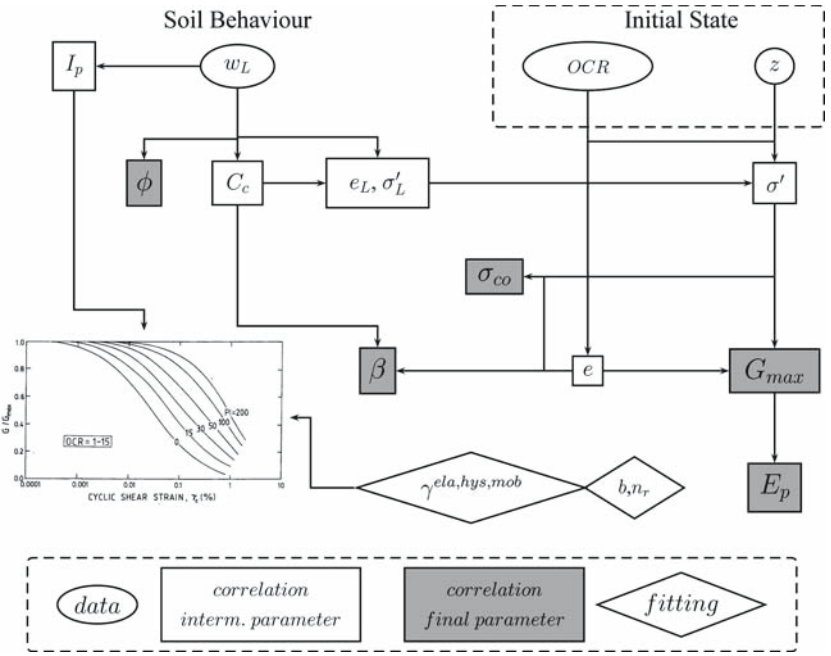

Fig. 8 Methodology for elastoplastic model parameter identification of clays

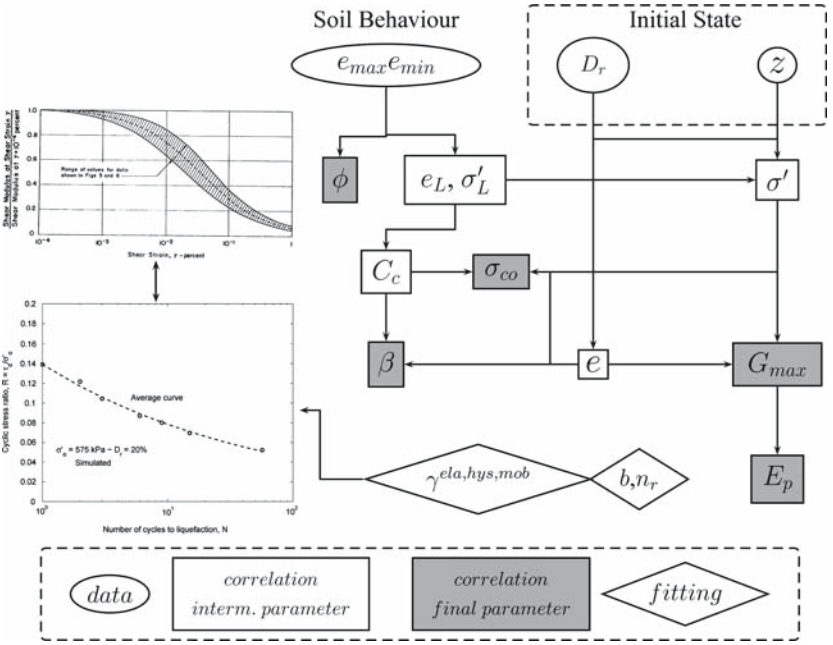

Fig. 9 Methodology for elastoplastic model parameter identification of sands

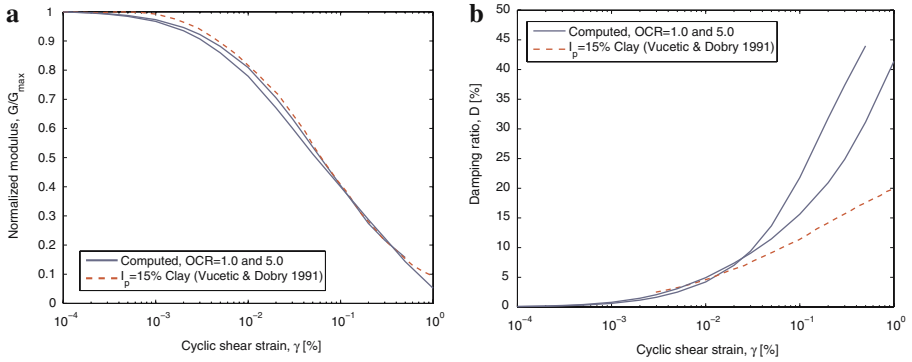

Fig. 10 Comparison between simulated and Vucetic and Dobry [1991] reference curves for $I_p = 15\%$ clay model : **a** $G/G_{\max} - \gamma$ and **b** $D - \gamma$

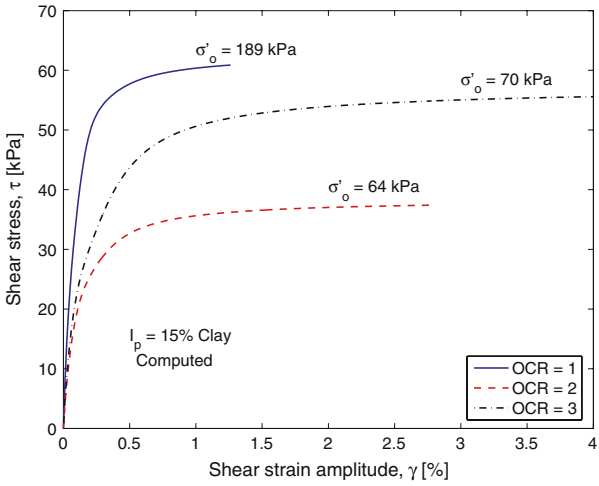

Fig. 11 Simulated variation of shear stress τ with shear strain γ for three undrained simple monotonic shear tests. $I_p = 15\%$ clay model

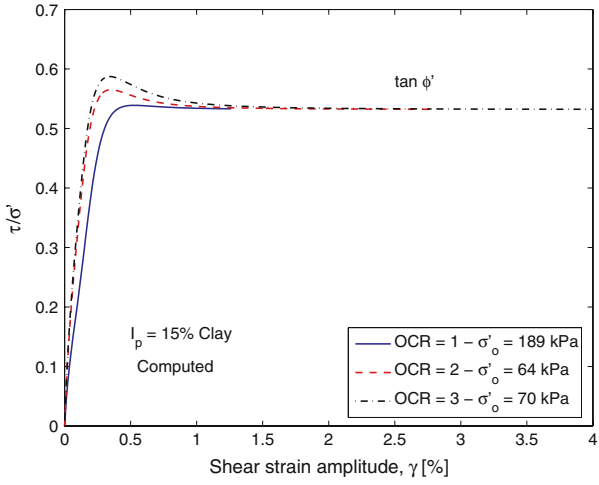

Fig. 12 Simulated variation of τ/σ' with shear strain γ for three undrained simple monotonic shear tests. $I_p = 15\%$ clay model

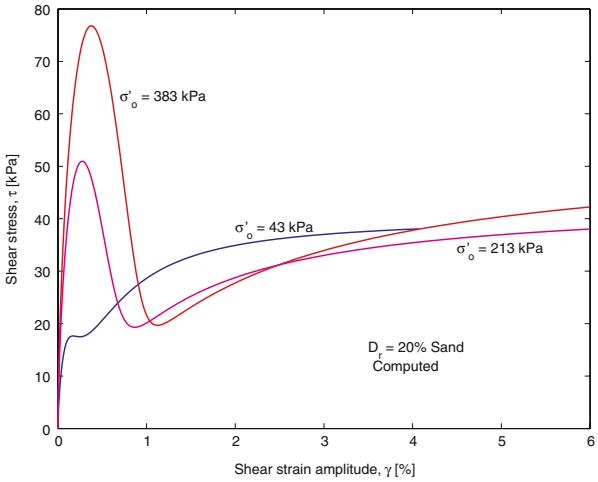

Fig. 13 Simulated variation of shear stress τ with shear strain γ for three undrained simple monotonic shear tests. $D_r = 20\%$ sand model

such tests obtained in the $\tau - \gamma$ plane. In order to verify the validity of the proposed model parameters, we have plotted the variation of the (τ/σ') ratio with respect to the shear strain (γ) in Fig. 12. It shows that the soil behaviour is always contracting when OCR $= 1$ and dilating for OCR > 1, where the material exceeds the critical state line before reaching perfect plasticity. Therefore, for overconsolidated material, resistance degradation is also modeled. In addition, the comparison of the S_u-values obtained in the numerical simulation are in perfect coherence with the empirical correlations, as for example, that given by Jamiolkowski et al. [1985]:

$$\frac{S_u}{\sigma'} = (0.23 \pm 0.04)\mathrm{OCR}^{0.8}, \tag{23}$$

where σ'_m is the initial vertical effective stress. In the simulation, S_u/σ', values of 0.34, 0.60 and 0.80 are obtained for OCR of 1.0, 2.0 and 3.0, respectively.

4.2 Tests for sands

In this section, a unique type of sand with different D_r at several initial confining pressures is studied. The main characteristics of the sand used are as follows: $C_u = 1,3$, $C_z = 1.0$, $e_{\min} = 0.58$ and $e_{\max} = 0.98$. Once the parameters are estimated, undrained cyclic strain-controlled shear tests are simulated to verify the coherence of the parameters.

Figures 13 and 14 show the response obtained by the model with $D_r = 20\%$ for the monotonic test in the τ–γ and τ-σ' planes.

Figure 15 shows the simulated response of a drained cyclic strain-controlled shear test for the sand at $D_r = 40\%$ and two σ' (20 and 300kPa). The obtained $G/G_{\max}$–γ and $D - \gamma$ curves are compared to the reference curves given by Kokusho [1980] for sands at the same initial pressure. As can be noticed, the $G/G_{\max} - \gamma$ curves match relatively well for both σ'-values. Nevertheless, for strains larger than 0.01%, the damping ratio D is over-estimated.

In the case of sands, the cyclic tests are related principally to the study of liquefaction problems. In order to characterize the liquefaction resistance of a sand with $D_r = 20\%$, undrained cyclic shear tests were simulated. Both approaches, stress

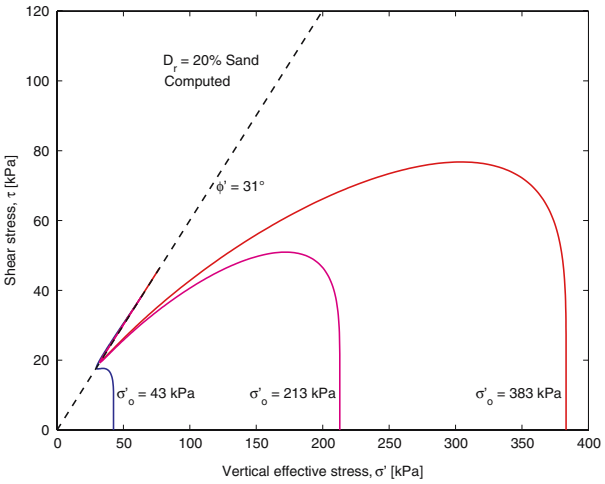

Fig. 14 Simulated variation of shear stress τ with normal stress σ' for three undrained simple monotonic shear tests. $D_r = 20\%$ sand model

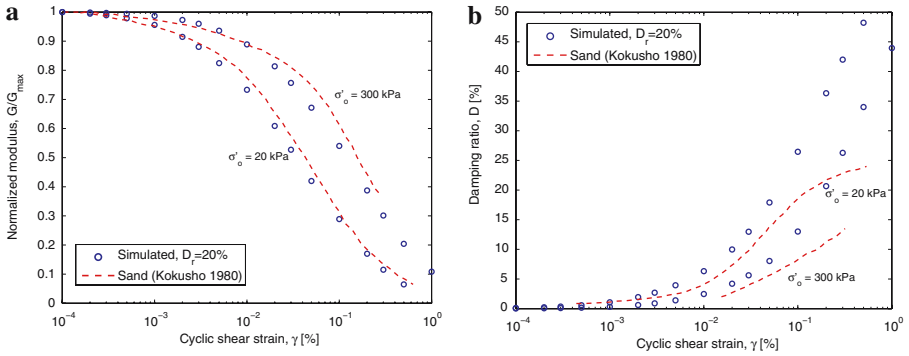

Fig. 15 Comparison between simulated and Kokusho [1980] reference curves for sand $D_r = 20\%$ model : **a** $G/G_{\max} - \gamma$ and **b** $D - \gamma$

controlled and strain controlled, were used. The first one gives a curve of cyclic stress ratio ($R = \tau_d/\sigma'$) as a function of the number of loading cycles to produce liquefaction (N) (Fig. 16). The second approach, proposed by Dobry et al. [1982], produces a curve of pore pressure ratio ($r_u = \Delta U/\sigma'$) after 10 cycles as a function of cyclic strain (Fig. 17). According to these figures, the model responses for both loading paths are coherent for the same initial conditions (i.e. D_r and σ') and both of them can be used to validate the model.

5 Numerical application

5.1 Cohesive soil deposits

To illustrate the effects that overconsolidation ratios OCR have on surface seismic response, a generalized typical layered soil/rock model is considered in this section. The soil deposit is assumed to be a clay layered profile, with a thickness of 36 m over

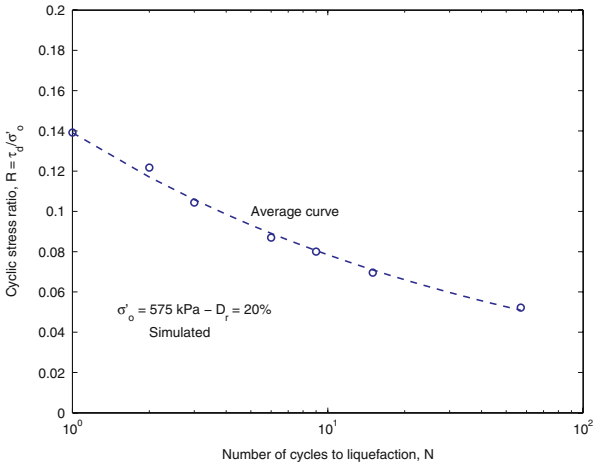

Fig. 16 Simulated $D_r = 20\%$ sand model liquefaction curves, stress controlled tests

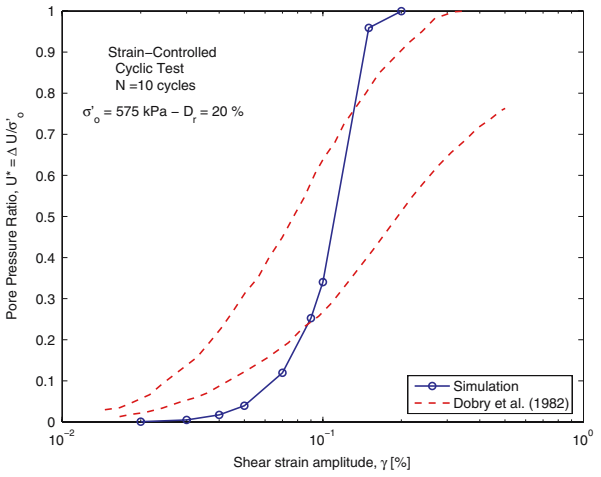

Fig. 17 Simulated $D_r = 20\%$ sand model liquefaction curves, strain controlled tests

the bedrock. The shear wave velocity profile is shown in Fig. 18. The shear wave velocity profile gives an average shear wave velocity in the upper 30 m (V_{s30}) of 200 m/s, corresponding to a site category C of Eurocode 8. The fundamental elastic period of the soil profile is 0.67 s.

The profile is composed of clays with I_p equal to 15%. The soil profile is considered homogeneous and three different OCR-values (i.e. 1.0, 2.0 and 3.0) are used. Even if the V_s-value used for the three cases is the same, only the initial state (OCR) is changed in order to illustrate its influence on the seismic response of the profile.

A deformable bedrock with a shear wave velocity of 500 m/s is placed at 36 m depth.

The methodology explained in this paper is used to determine the soil model parameters. In this case, the Darendeli [2001] curves for $I_p = 15\%$ clay have been used as "measured" curves.

Figure 19 shows the model prediction for the variation of $G/G_{\max}$ with the cyclic shear strain γ in undrained strain-controlled cyclic direct simple shear tests at two

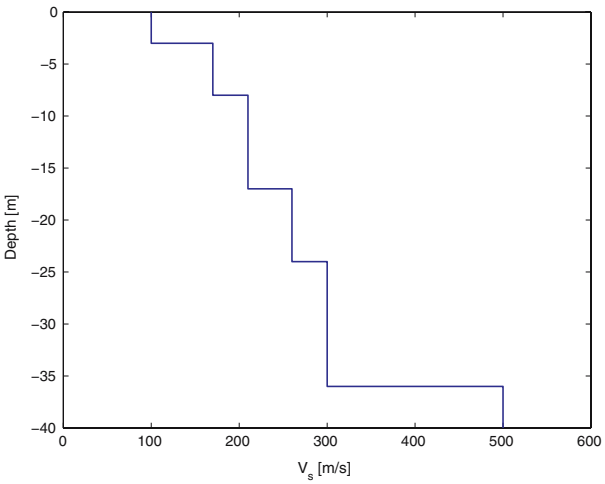

Fig. 18 Soil profile characterization

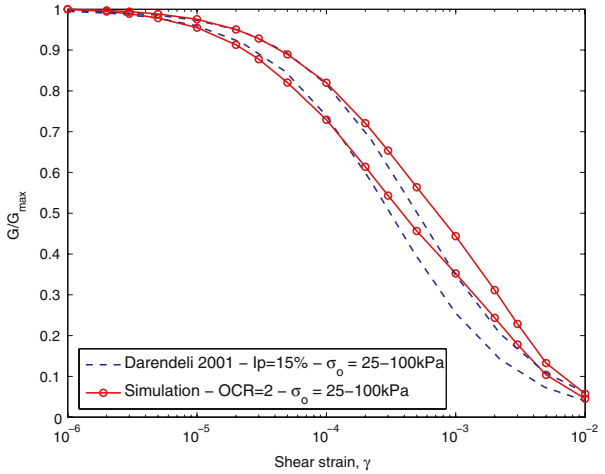

Fig. 19 Comparison between simulated $G/G_{\max} - \gamma$ and Darendeli [2001] reference curves for $I_p = 15\%$ clay model

initial confining pressures ($\sigma'_o = 25$ and 100 kPa). These curves are compared with the modulus reduction curve given by Darendeli [2001] for $I_p = 15\%$ clay.

The used seismic input motions are the acceleration records of Friuli earthquake–San-Rocco site (Italy-1976) and Superstition Hills earthquake–Supers. Mountain site (USA-1987). These signals are consistent with the response spectra of Type A soil (i.e. rock) of Eurocode8. The response of the site profile is computed using only the horizontal component of the input records.

In as far as it concerns the acceleration history obtained in our analyses, the effect of the-OCR value of the soil profile on the obtained acceleration at the surface level (PGA_{surf}) is studied.

In practice, the most common approach to estimate the PGA_{surf} value is to use attenuation relationships such as those given by Idriss [1991] or Dickenson and Seed [1996]. These relations take into account the influence of the non linearity of soil behaviour on the obtained PGA_{surf} value. Figure 20 shows the variation of peak

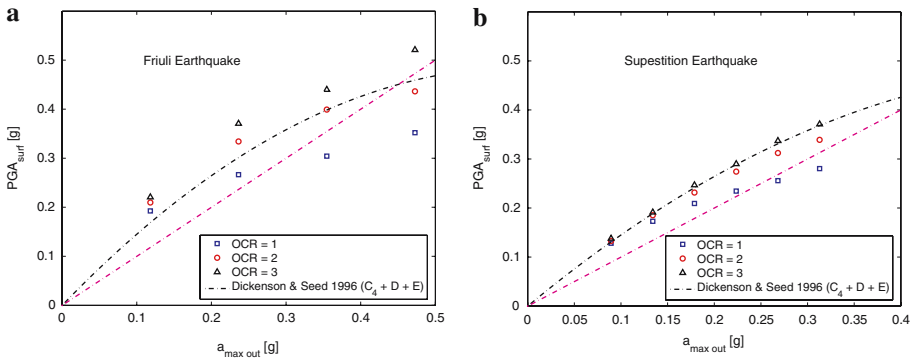

Fig. 20 Relationships between maximum acceleration on bedrock and surface obtained in the soil profile for different earthquakes : **a** Friuli earthquake and **b** Superstition earthquake

ground acceleration at the surface (PGA_{surf}) as a function of the maximum acceleration at the outcropping bedrock ($a_{max\ out}$). According to this figure, the amplification of peak ground acceleration on the ground surface relative to bedrock appears for $a_{max\ out}$ value to be less than 0.25g in the case of normally consolidated soil behaviour (i.e. OCR = 1). Furthermore, these responses illustrate that the estimated PGA_{surf} values for the model with OCR = 1 are much smaller than those obtained for OCR = 2 and 3.

This variation is due to the difference in the "rigid" behaviour of overconsolidated soils even if the V_s profiles and $G/G_{max} - \gamma$ curves are similar.

6 Conclusions

A consistent and coherent methodology to determine an elastoplastic model parameters for clayey and sandy soils has been proposed. For clays, Atterberg limits and an OCR ratio can be used to identify the mechanical parameters, while for sands, the relative density or the void ratio is the dominant parameter.

This methodology, which can form the basis for a decision making process, has two aims. First, to give a handy, easy-to-obtain and coherent set of parameters to use when no experimental data is available. Second, to be used as the starting point for cases where geotechnical measurements are not sufficient.

In the numerical applications, the importance of all model parameters and the differences that the errors on their identification can induce in the seismic site response were illustrated.

In the companion paper, this methodology is generalized to natural soil in order to evaluate the seismic response of real sites subjected to natural acceleration records.

Acknowledgements A part of this study has been done in the framework of the European Community Contract No ENV-CT97- 0392.

References

Anastasiadis JA, Pitilakis KD (1996) Shear modulus G_o and damping of typical Greek soils at low strain amplitudes. Tech Chron Sci J TCG 16(3):9–18

Aubry D, Hujeux J-C, Lassoudire F, Meimon Y (1982) A double memory model with multiple mechanisms for cyclic soil behaviour. In: Proceedings of the International Symposium Num. Mod. Geomech, Balkema, pp 3–13

Aubry D, Modaressi A, Modaressi H (1990) A constitutive model for cyclic behaviour of interfaces with variable dilatancy. Comput Geotechnics 9(1/2):47–58

Bardet J-P (1997) Experimental soil mechanics. Prentice Hall, Upper Saddle River, NJ

Been K, Jefferies MG (1985) A state parameter for sands. Géotechnique 35(2):99–112

Biarez J, Favre J-L (1972) Corrélations de paramètres en mécanique des sols. Table ronde nationale, Ecole Centrale Paris

Biarez J, Hicher P-Y (1994) Elementary mechanics of soil behaviour, saturated and remolded soils. Balkema, Amsterdam, The Netherlands

Darendeli MB (2001) Development of a new family of normalized modulus reduction and material damping curves. Ph.D. Dissertation, University of Texas at Austin, USA

Dickenson SE, Seed RB (1996) Non-linear dynamic response of soft and deep cohesive soil deposits. In: Proceedings of the international workshop on site response subjected to strong earthquake motions, vol 2. Yokosuka, Japan, pp 67–81

Dobry R, Ladd RS, Yokel FY, Chung RM, Powell D (1982) Prediction of pore water pressure buildup and liquefaction of sands during earthquakes by the cyclic strain method. Nat Bur Stand Build Sci Ser 138:11–49

Favre J-L (1980) Milieu continu et milieu discontinu: mesure statistique indirecte des paramètres rhéologiques et approche probabiliste de la sécurité. Thèse de docteur ès sciences, Univ. Pierre et Marie Curie, Paris VI, France

Ghaboussi J., Dikmen SU (1978) Liquefaction analysis of horizontally layered sands. J Geotechn Eng Div ASCE 104(nr GT3):341–356

Hardin BO (1978) The nature of stress-strain behavior for soils. In: Proceedings ASCE geotechnical engineering division. Specially conference on earthquake engineering and soil dynamics, vol.1 Pasadena, CA, pp 3–89

Hicher P.Y, Rahma A (1994) Micro-macro correlations for granular media. Application to the modelling of sands. Eur J Mechanics A/Solids 13(6):763–781

Hujeux J-C (1985) Une loi de comportement pour le chargement cyclique des sols. In: Davidovici V, (ed) Génie Parasismique. Presses ENPC, France, pp 278–302

Idriss IM (1991) Earthquake ground motions at soft soil sites. In: Prakash S (ed) Proceedings of the 2nd international conference on recent advances in geotechnical earthquake engineering and soil dynamics, vol 3. St. Louis, Missouri, pp 2265–2271

Ishibashi I, Zhang X (1993) Unified dynamic shear moduli and damping ratios of sand and clay. Soils Found 33(1):182–191

Ishihara K (1993) Liquefaction and flow failure during earthquakes. 33rd Rankine lecture. Géotechnique 43(3):351–415

Ishihara K, Tatsuoka F, Yasuda S (1975) Undrained deformation and liquefaction of sand under cyclic stresses. Soils Found 15(1):29–44

Iwasaki T, Tatsuoka F, Takagi Y (1978) Shear moduli of sands under cyclic torsional shear loading. Soils Found 18(1):39–56

Jamiolkowski M, Ladd CC, Germaine JT, Lancellotta R (1985) New developments in field and laboratory testing of soils. In: Proceedings of the 11th international conference on soil mechanics and foundations engineering, vol 1. San Francisco, CA, pp 57–154

Kallioglou P, Tika Th, Pitilakis K (1999) Dynamic characteristics of natural cohesive soils. In: Proceedings of the 2nd international conference on earthquake geotechnical engineering. Lisbon, Portugal

Kohata Y, Tatsuoka F, Wang L, Jiang GL, Hoque E, Kodaka T (1997) Modelling the non-linear deformation properties of stiff geomaterials. Symposium in print. Géotechnique 47(3):563–580

Kokusho T (1980) Cyclic triaxial test of dynamic soil properties for wide strain range. Soils Found 20(4):45–60

Kokusho T, Yoshida Y, Esashi Y (1982) Dynamic properties of soft clays for wide strain range. Soils Found 22(4):1–18

Kramer SL (1996) Geotechnical earthquake engineering. Prentice Hall, Upper Saddle River, NJ

Mellal A (1997) Analyse des effets du comportement non linéaire des sols sur le mouvement sismique. Thèse de doctorat, École Centrale Paris, France
Modaressi H, Foerster E (2000) CyberQuake. User's manual, BRGM, France
Pande GN, Pietruszczak S, (1986) A critical look at constitutive models for soils. In: Dungar R, Studer JA (ed) Geomechanical modelling in engineering practice. Balkema AA, Rotterdam, The Netherlands, pp 369–395
Prévost J-H, Hoeg K (1975) Effective stress-strain strength model for soils. J Geotechnical Eng Div ASCE 101(nr GT3):259–278
Saim R (1997) Dès comportements repères des grains sans colle à un exemple de sol réel. Thèse de doctorat, École Centrale Paris, France
Santos JA (1999) Caracterização de solos através de ensaios dinâmicos e cíclicos de torção ; Aplicação ao estudo do comportamento de estacas sob acções horizontais estáticas e dinâmicas. Dissertação Doutor, Universidade Técnica de Lisboa, Instituto Superior Técnico, Portugal
Schofield AN, Wroth CP (1968) Critical state soil mechanics. McGraw-Hill, London
Seed HB, Idriss IM (1970) Soil moduli and damping factors for dynamic response analyses. University of California, Berkeley, CA, Report EERC-70-10, Earthquake Engineering Research Center
Seed HB, Wong RT, Idriss IM, Tokimatsu K (1986) Moduli and damping factors for dynamic analyses of cohesionless soils. J Geotechnical Eng ASCE 112(11):1016–1032
Sun JI, Golesorkhi R, Seed HB (1988) Dynamic moduli and damping ratios for cohesive soils. University of California, Berkeley, CA, EERC-88-15
Vucetic M (1994) Cyclic threshold shear strains in soils. J Geotechnical Eng ASCE 120(12):2208–2228
Vucetic M, Dobry R (1991) Effect of soil plasticity on cyclic response. J Geotechnical Eng ASCE 117(1):89–107